Dyes and Pigments 99 (2013) 759–770

Contents lists available at SciVerse ScienceDirect

Dyes and Pigments

journal homepage: www.elsevier.com/locate/dyepig

Confinement of 5,10,15,20-tetrakis-(4-sulfonatophenyl)-porphyrin in novel poly(vinylpyrrolidone)s modified with aromatic amines

Myriam Gómez-Tardajos [a], Juan Pablo Pino-Pinto [b], Claudia Díaz-Soto [b], Mario E. Flores [c], Alberto Gallardo [a], Carlos Elvira [a], Helmut Reinecke [a], Hiroyuki Nishide [d], Ignacio Moreno-Villoslada [b,*]

[a] Instituto de Ciencia y Tecnología de Polímeros, ICTP-CSIC, Juan de la Cierva 3, 28006 Madrid, Spain
[b] Instituto de Ciencias Químicas, Facultad de Ciencias, Universidad Austral de Chile, Casilla 567, Valdivia, Chile
[c] Departamento de Ciencias de los Materiales, Facultad de Ciencias Físicas y Matemáticas, Universidad de Chile, Casilla 567, Santiago, Chile
[d] Department of Applied Chemistry, School of Science and Engineering, Waseda University, Tokyo 169-8555, Japan

ARTICLE INFO

Article history:
Received 13 February 2013
Received in revised form
19 June 2013
Accepted 21 June 2013
Available online 28 June 2013

Keywords:
Porphyrins
Polymer–dye interactions
Confinement of dyes in nanoparticles
Aromatic–aromatic interactions
Preferential solvation
Amphiphilic properties

ABSTRACT

Polymeric derivatives of the biocompatible poly(vinylpyrrolidone) bearing discrete amounts of aromatic amines have been synthesized. The interaction of 5,10,15,20-tetrakis-(4-sulfonatophenyl)-porphyrin with a series of these copolymers (P10, P25, P50, P75, and P100, the numbers referring the molar percentage of incorporation of aromatic amines in the copolymers) has been analyzed regarding shifts of the absorption bands and shift of the transition pH between the di-anionic and the tetra-anionic forms of 5,10,15,20-tetrakis-(4-sulfonatophenyl)-porphyrin. The interaction between the dye and poly(-vinylpyrrolidone) has also been studied as a control. The incorporated aromatic amines increase the hydrophobic properties of the resulting polymers and provide specific interactions with the tetra-anionic form of 5,10,15,20-tetrakis-(4-sulfonatophenyl)-porphyrin. Thus, P10 was soluble in water, P25 was dispersible in the form of polydisperse nanoparticles, and P50, P75, and P100 are insoluble in water. However, low polydisperse nanoparticles of mean size of 175 nm were formed by pouring 1 volume of a solution of P25 in DMSO into 9 volumes of water. These nanoparticles are permeable to 5,10,15,20-tetrakis-(4-sulfonatophenyl)-porphyrin. Both P10 and P25 nanoparticles produce strong binding to 5,10,15,20-tetrakis-(4-sulfonatophenyl)-porphyrin, stabilize the tetra-anionic form of the dye in a wide range of pH, and prevent the undesirable self-aggregation both in the form of H- and J-aggregates. It was shown that the affinity of the 5,10,15,20-tetrakis-(4-sulfonatophenyl)-porphyrin for P10 is stronger than for chitosan, which gives insights concerning the possible stability of the complex in biological systems.

1. Introduction

Porphyrins have increased their applications over the last years due to their efficiency in photodynamic therapy (PDT) in cancer [1]. PDT is a combined light-plus-drug treatment for malignant tumors. The PDT drug Photofrin®, a water-soluble, red powder consisting of a mixture of metal-free porphyrins, is approved in the U.S. for treatment of obstructing cancer of the esophagus and early stage cancer of the bronchus [2]. Clinical trials are reported for tumors of the skin, brain, head and neck, urinary bladder, gastro-intestinal tract, and female genital tract. PDT is based on the cell damage induced by the oxygen in the tumor tissues [3]. The active molecule in PDT is singlet oxygen which is generated by means of the energy given upon relaxation of a dye (photosensitizer) from an excited state [4,5]. The photodynamic action of any photosensitizer in biological systems is a puzzle which is strongly influenced by the environmental conditions of the dye, including photosensitizer location and interactions, photosensitizer self-aggregation, reactivity of surrounding molecules and biological targets, as well as diffusion kinetics, and life-times of excited states, factors that can be determinant in the photodynamical mechanism and efficiency of the therapy [6]. Robust methods that ensure a high efficiency of singlet oxygen production are desirable. Controlling the environmental characteristics of photosensitizers is one strategy that may enhance singlet oxygen production. Confinement in polymeric matrices or micelles as carriers may be one strategy to control the dye environment [7–9]. The desired properties of these carriers may comprise the stability of the active triplet excited state of the

* Corresponding author. Fax: +56 63 293520.
E-mail address: imorenovilloslada@uach.cl (I. Moreno-Villoslada).

0143-7208/$ – see front matter © 2013 Elsevier Ltd. All rights reserved.
http://dx.doi.org/10.1016/j.dyepig.2013.06.028

dye, avoidance the dye self-aggregation in order not to disperse the energy but produce reaction with triplet oxygen, and improvement of the tumor targeting.

Regarding these biomedical applications, searching biocompatible polymers to achieve a control of the dye environment is of interest. Poly(vinylpyrrolidone) (PVP) is a non-ionic, water soluble polymer, extensively used for biomedical applications and in cosmetics, personal hygiene, and contact lenses fabrication due to its non-toxicity [10]. It has been approved by the FDA as a nutritional additive and it is also used as stabilizer (E1201). This polymer has also recognized amphiphilic properties, and has been used as surfactant [11,12] and stabilizer in dispersion polymerization reactions, obtaining microspheres of controlled size [13–15]. An adequate functionalization strategy of this polymer opens huge possibilities for different applications. We have previously described the synthesis of a functional vinylpyrrolidone (VP) modified with different groups such as aromatic amines [16] (VP–$ArNH_2$). Aromatic amines are useful for increasing the hydrophobia of PVP derivatives, and may produce aromatic–aromatic interactions with aromatic molecules [17]. Close binding between the aromatic species allows short-range electrostatic interactions taking place between two aromatic groups, which define the geometry of the assembly [18,19]. Indeed, aromatic–aromatic interactions may be enhanced when both aromatic groups present complementary charges. We have shown that the extent of binding and the state of aggregation of different dyes in the presence of polyelectrolytes strongly depend on the structure of the polymer as a whole, and other variables such as functional groups, localization of the charge, flexibility, hydrophobia, linear charge density, and linear aromatic density seem to determine the behavior of the system [20–29]. The copolymerization of pure VP and VP–$ArNH_2$ may produce copolymers with different linear aromatic amine density, allowing modulation of the properties of the polymer in order to achieve a better control of the dye environment, providing a potential application for PDT.

5,10,15,20-Tetrakis-(4-sulfonatophenyl)-porphyrin (TPPS) is a photosensitizer whose physicochemical properties allow exploration of their close environment. It presents acid and base forms whose equilibrium is sensitive to environmental conditions [30]. The transition between the basic, tetra-anionic form of TPPS (H_2TPPS^{4-}) to the acid, di-anionic form of the dye (H_4TPPS^{2-}) is easily followed by UV–vis spectroscopy. It also presents solvatochromic properties [31], and undergoes preferential solvation for polar organic solvents, as such described for DMSO in mixtures water:DMSO [31]. Besides, its state of aggregation produces changes on the electronic transitions that can be also followed by UV–vis spectroscopy [26,32]. In this paper, the synthesis of copolymers of VP and VP–$ArNH_2$ will be shown, and their interaction with TPPS will be studied by UV–vis spectroscopy. The interaction between TPPS and PVP will also be studied as a control. The possibility of confinement of TPPS in polymeric complexes and nanostructures will be analyzed.

2. Experimental

2.1. Materials

VP (Sigma–Aldrich) was purified by distillation at low pressure. Isatoic anhydride (Sigma–Aldrich) and lithium diisopropylamide (LDA) (Sigma–Aldrich) were used to synthesize VP–$ArNH_2$. Azoisobutyronitrile (AIBN, Sigma–Aldrich) was recrystallized from ethanol and used as polymer synthesis initiator. TPPS (TCI) was used without further purification for interaction studies. Dimethylformamide (DMF, Sigma–Aldrich), dimethylsulfoxide (DMSO, Merck), acetonitrile (Merck), ethanol (Merck), deionized, distilled water, deuterated dimethylsulfoxide (DMSO-d_6, Sigma–Aldrich), and deuterated water (D_2O, Sigma–Aldrich) were used as solvents. The pH was adjusted with minimum amounts of HCl (Fisher Scientific) and NaOH (Sudelab). Tetramethylsilane (TMS, Sigma–Aldrich) was used as internal standard for NMR analyses. Pyrene (Sigma–Aldrich) was used as a probe for micelle formation after being twice recrystallized from ethanol. Monodisperse standard poly(styrene) (Polymer Laboratories) was used for molecular mass calculations. Chitosan (CS, Protasan, deacetylation degree >80%, NovaMatrix) and PVP of Mw of 30,000 (Merck) and 1,300,000 g/mol (Sigma–Aldrich) were used for comparative studies. The structures of the polymers and TPPS in both its basic and acid forms are shown in Fig. 1.

2.2. Equipment

Distilled water was deionized in a Simplicity Millipore deionizer. The pH was controlled on an UltraBasic Denver Instrument pH meter. UV–vis measurements were performed in a Heλios γ spectrophotometer. ^1H NMR spectra were recorded on a Bruker Avance-300 NMR apparatus. Size exclusion chromatography (SEC) was done using a Perkin–Elmer apparatus with an isocratic pump connected to a differential refractometric detector (serial200a). Fluorescence was analyzed in a SCINCO FluoroMate FS-2spectrometer. Apparent size and zeta potential of suspended nanoparticles were obtained by dynamic light scattering (DLS) on a Malvern Zetasizer Nano ZS (Malvern) instrument with backscatter detection (173°), controlled by the Dispersion Technology Software (DTS 6.2, Malvern).

2.3. Procedures

2.3.1. Polymer synthesis

The synthesis of VP–$ArNH_2$ was accomplished following the method previously described [16], and shown in Scheme 1. Monomers (VP and VP–$ArNH_2$) and the initiator AIBN were dissolved in DMF at total monomer concentration of 1 M and initiator concentration of $1.5 \cdot 10^{-2}$ M. Nitrogen was flushed through the polymerizing solution for 30 min. Polymerizations were carried out at 60 °C during 24 h. The formed copolymers were isolated and purified by dialysis (Slide-A-Lyser 3.5K Dialysis Cassette, 3500 molecular weight cutoff, PIERCE) against mixtures deionized water:DMF for 24 h and then against deionized water for 48 h to minimize the presence of residual unreacted monomers and other low molecular-weight molecules. Structural characterization of the polymers was carried out by NMR in DMSO-d_6 using the MestreNova© 6 software. Chemical shifts are given in the δ scale relative to TMS. The molecular weight was analyzed by SEC. Two ResiPore™ columns (Varian) were conditioned at 70 °C and used to elute the samples (1 mg/ml) with HPLC-Grade DMF supplemented with 0.1% v/v LiBr at a rate of 1 ml/min. Calibration of SEC apparatus was carried out with monodisperse standard poly(styrene) samples in the range of $2.9 \cdot 10^3$–$480 \cdot 10^3$ Da.

2.3.2. Interaction studies

Absorption UV–vis analyses were performed using quartz vessels with path lengths of 1 cm following conventional procedures. Particular experimental conditions are provided in the captions of Figs. 2–12. The polymer concentrations are given in mole of aromatic basic groups per liter for polymers containing amine groups or in mole of monomeric units per liter for PVP. All samples were prepared in pure water or mixtures of water:DMSO 90:10 and allowed to equilibrate after pH adjustment for several minutes. In the latter case, the polymers were dissolved in pure DMSO and then

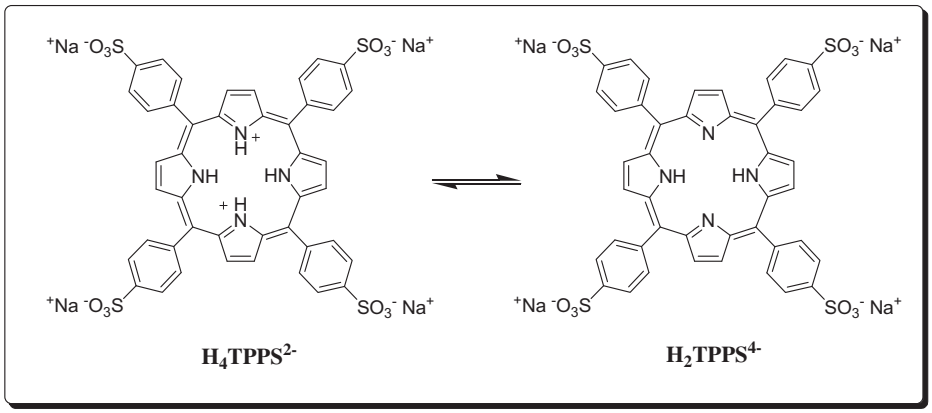

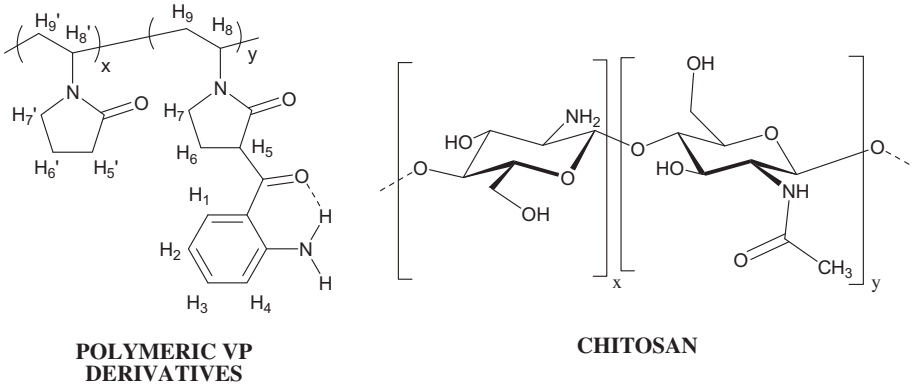

Fig. 1. Molecular structures. For the polymeric VP derivatives, PVP corresponds to $x = 1$, $y = 0$, and P10, P25, P50, P75, and P100 are the polymers for which the numbers represents the value of y (%); for chitosan, $x > 0.85$; TPPS is shown in its acid and its base forms.

1 volume of the DMSO solution was added to 9 volumes of aqueous solutions either containing or not containing TPPS.

2.3.3. Nano- and microparticle formation and analysis

Samples containing $9 \cdot 10^{-5}$ M of the corresponding polymers in water:DMSO 90:10 and variable TPPS concentrations were prepared by pouring a polymer solution in DMSO into an aqueous solution containing the dye at pH 3.5 under vigorous stirring and analyzed at 298 K by DLS to obtain the size and the zeta potential of the particles formed. Results of size and zeta potential were considered valid under the criteria of the DTS 6.2 software. The formation of nano- and micro-particles with PVP, in the presence or not of TPPS, was searched by DLS and fluorescence spectroscopy using pyrene as probe. For fluorescence studies of the PVP solutions containing pyrene, the excitation wavelength was fixed to 320 nm and the emission was analyzed between 350 and 500 nm. Slits of excitation and emission were fixed to 2.5 nm and pyrene concentration was fixed at $1 \cdot 10^{-5}$ M.

3. Results and discussion

3.1. Polymer synthesis and physicochemical properties

Statistical copolymers (P10, P25, P50, P75, and P100) with increasing amount of VP–$ArNH_2$ were obtained by free radical polymerization. Table 1 shows the copolymer composition, molecular weight, and polydispersity index (PDI) obtained for each synthesis. The acronyms of the copolymers are given as an indication of the molar fraction of VP–$ArNH_2$ in the feed, which practically corresponds to the actual value of the molar co-monomeric composition. The analysis of the composition of the different copolymers was carried out by comparison of the integrated areas (A) of proton resonance signals of the corresponding spectra, which are shown in Fig. 2, considering chemical shifts ranges between 7.0 and 8.0 ppm, corresponding to aromatic protons H_1 and H_3 and NH_2 of aniline, and 1.0–2.4 ppm corresponding to the more shielded methylene protons H_6, H_9, H'_5, H'_6, and H'_9 (see Figs. 1 and 2 for assignments). The corresponding molar fractions ($x = f_{VP}$; $y = f_{VP-ArNH_2}$) are calculated using Equations (1)–(5), where H is the integrated area for a single proton:

$$A_{1.0-2.4} = 4Hf_{VP-ArNH_2} + 6Hf_{VP} \quad (1)$$

$$A_{7.0-8.0} = 4Hf_{VP-ArNH_2} \quad (2)$$

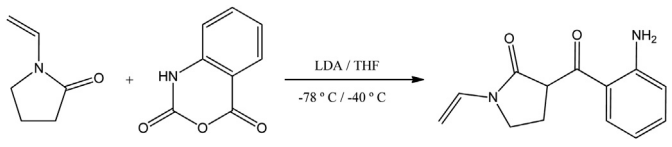

Scheme 1. Chemical reaction for VP derivatization.

Table 1
Copolymer composition related to feed composition and the resulting molecular weight (MWn) and polydispersity index (PDI).

Polymer	$f_{VP-ArNH_2}$ in the feed	$f_{VP-ArNH_2}$ in the polymer	MWn (kDa)/PDI
P10	0.10	0.08	33/1.60
P25	0.25	0.23	41/1.62
P50	0.50	0.46	43/1.81
P75	0.75	0.74	34/1.77
P100	1	1	41/1.86

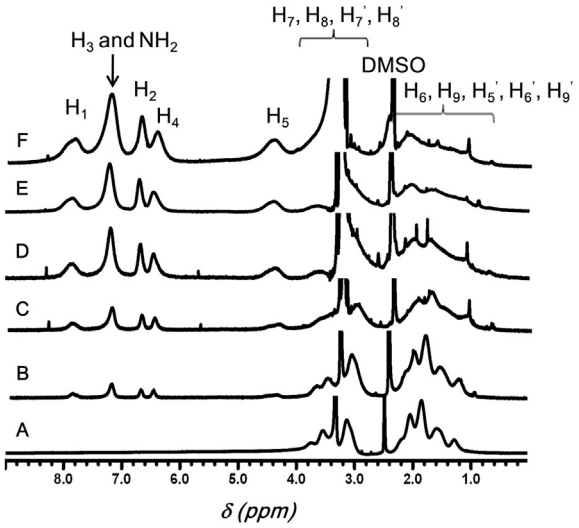

Fig. 2. 300 MHz ^{1}H NMR spectra of PVP (A), P10 (B), P25 (C), P50 (D), P75 (E), and P100 (F) in DMSO.

$$f_{VP-ArNH_2} = 1 - f_{VP} \tag{3}$$

Dividing (1) by (2), and rearranging, we obtain

$$f_{VP} = \frac{\frac{4}{6}\left(\frac{A_{1.0-2.4}}{A_{7.0-8.0}} - 1\right)}{1 + \frac{4}{6}\left(\frac{A_{1.0-2.4}}{A_{7.0-8.0}} - 1\right)} \tag{4}$$

and

$$f_{VP-ArNH_2} = \frac{1}{1 + \frac{4}{6}\left(\frac{A_{1.0-2.4}}{A_{7.0-8.0}} - 1\right)} \tag{5}$$

Protonation of the amino groups should increase the hydrophilia of the polymers and allow their dissolution in water, so that, in the copolymers hereby reported, as the linear aromatic amine density increases from P10 to P100, an increase on their solubility in water in acid media was expected. However, the opposite behavior was experimentally observed, that is, the solubility in water of the copolymers decreases as the amount of VP–ArNH$_2$ increases even at acid conditions. Aniline is a basic molecule whose pK_a has been reported to be near 4.6. Withdrawing substituents make the pK_a decrease, and values around 3.0 have been reported [33]. We investigated the behavior of P10 at a concentration of 0.1 M in D_2O versus the pH by ^{1}H NMR spectroscopy. It can be seen in Fig. 3 left, that protons H_2 and H_4, which in this solvent appeared overlapped, are the most sensitive to the pH change due to they are in *para* and *ortho* position, respectively, with respect to the amino group. Note that protons at the amino group are not observed in this solvent due to fast exchange with deuterium. As deduced from the graph in Fig. 3 right, where the chemical shifts of protons H_2 and H_4 are plotted versus the pH, protonation of the amino groups begins at pH around 3, and, as recurrent in ionizable polymers, gradually increases as the pH decreases. Consider, however, that upon diluting, or in the presence of anions that stabilize the positive charges, the probability of the copolymers to protonate may increase. Apart from the withdrawing effect of the carbonyl group, a stabilization of a resonance form of the aromatic amine in which the amine is establishing a hydrogen bond with the neighboring carbonyl group, as depicted in Fig. 1, may produce a decrease on the basicity of the nitrogen atom. The planar configuration of the aromatic pendant groups may enhance their self-stacking and confinement in hydrophobic domains of the polymer, a fact whose probability increases with the increase on the linear aromatic amine density in the copolymers. This could explain the decrease on the solubility of the copolymers bearing higher fractions of amino groups. Thus, PVP and P10 are readily water-soluble, P25 needs acid conditions to (apparently, see below) solubilize 10^{-4} M in water, and P50, P75, and P100 are insoluble in water.

All the polymers studied here are soluble in DMSO. However, the use of this solvent is a drawback for biological applications. Assays to find the minimum volume fraction of DMSO in water:DMSO mixtures to achieve solubility gave us an interesting result. All the copolymers appeared as soluble in water:DMSO 90:10 mixtures when pouring 1 volume of solutions of the copolymers in DMSO into 9 volumes of water at pH 3.5. However, the solubilization of P25, P50, P75, and P100 by this method resulted in colloidal suspensions as deduced by DLS experiments. The correlograms obtained by this technique are shown in Fig. 4. P10 is readily soluble in the mixture of solvents, so that low intense scattering is found. P50, P75, and P100 are found in the form of microparticles, showing a high PDI value and the presence of large particles as deduced from the noisy baseline. However, P25 is found in the form of nanoparticles of an apparent mean size of 175 nm, showing a low PDI value of 0.19, and a positive zeta potential of 9.23 mV that indicates the effective protonation of some aromatic amino residues at this pH. The zeta potential is low due to the low pK_a value of the substituted aniline and the low linear aromatic density (and hence linear charge density) of the polymer. Two explanations that do not exclude each other may be given to understand the role of DMSO in the process. Polymeric precipitates (nano-, micro-, or macro-metric) may appear by the well-known solvent displacement phenomenon when the solution of polymers in an organic, water-soluble solvent is poured into water [34,35]. Besides, DMSO may be intercalated between stacked

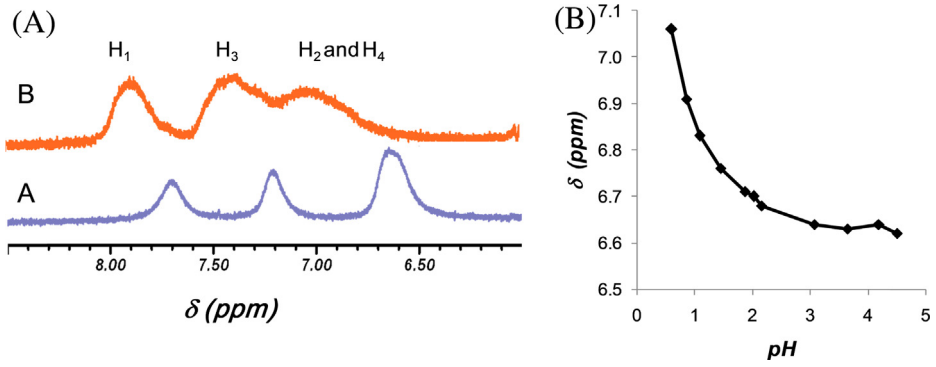

Fig. 3. Left: 300 MHz ^{1}H NMR spectra in D_2O of P10 at pH 3 (A) and 0.6 (B); right: chemical shift in ppm of protons H_2 and H_4 as a function of the pH.

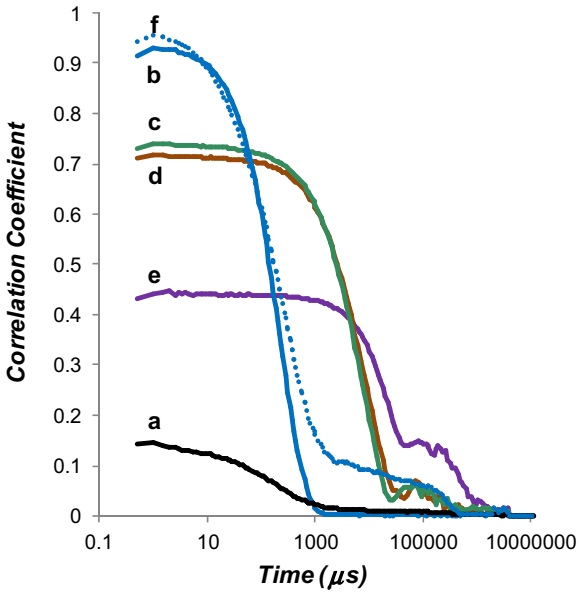

Fig. 4. Correlograms obtained by DLS in mixtures water:DMSO 90:10 for $9\cdot10^{-5}$ M of P10 (a), P25 (b), P50 (c), P75 (d), and P100 (e), and in water for $9\cdot10^{-5}$ M of P25 (f).

aromatic groups, solvating them, and generating microdomains rich in DMSO that may be stabilized by the VP moieties, so that preferential solvation of the aromatic amino groups could be also invoked to understand the enhanced solubilization of these polymers. Preferential solvation is attributed to a differentiation between the immediate surroundings of the solute and the composition of the bulk mixture, so that the local molar fraction of any co-solvent in the solute solvation shell appears to be higher than the molar fraction of this co-solvent in the bulk. This specific solvation arises due to differences in the specific and nonspecific interactions between the solute molecules and each of the solvent components [31]. In the case of the possible interaction between DMSO and the aromatic amines, π–π interactions may play an important role. Note that the DMSO ^{1}H NMR signal in Fig. 2 at around 2.5 ppm is shifted upfield in the presence of the aromatic amines; upfield shifting occurs when a molecule is sterically placed in the shielding cone of an aromatic group, revealing their close binding by means of specific interactions. The former mechanism may be more probable in the case of P50, P75, and P100, and the latter may be more probable in the case of P25, since, as will be discussed in the following sections, the microparticles obtained with P50, P75, and P100 were not permeable to TPPS, whilst the nanoparticles obtained with P25 were. On the other hand, the solubility of P25 in water was apparent, and colloidal suspensions were also found by DLS in pure water at pH 1, as can be also seen in Fig. 4, which showed higher PDI than when the polymer is previously dissolved in DMSO.

3.2. Acid–base and self-aggregation properties of TPPS

Many organic dyes such as TPPS have a tendency to self-stack due to aromatic–aromatic interactions stabilized by dispersion forces. In order to observe the formation of self-aggregates, UV–vis spectroscopy is a useful technique. The formation of aggregates in a sandwich-like disposition (H-aggregates) produces a shift of the absorbance maximum to higher energies. On the contrary, the formation of aggregates in a head-to-tail disposition (J-aggregates) produces a shift of the absorbance maximum to lower energies. Besides, H-aggregation produces fluorescence quenching, while J-aggregation produces aggregates that fluoresce [36–39].

In this respect, TPPS can undergo both H-type and J-type aggregation [26,40–43]. The latter case is found once the porphyrins are protonated at their pyrrole groups (see Fig. 1), forming a di-anionic species (H_4TPPS^{2-}), so that interaction between the positively charged center of the molecule with the negatively charged periphery stabilizes the aggregates. In this case, long arrangements of dyes slightly fold so that supramolecular polymers, coiling around an imaginary cylinder, have been described, as well as the induction of chirality in the presence of chiral seeds or asymmetric stirring [40,44]. This is reflected by the appearance of a band at around 490 nm, whilst the Soret band of the monomeric H_4TPPS^{2-} appears at 434–435 nm (see Fig. 5, continuous line and inset, and Table 2). H-type aggregates are normally found for the basic form of the dye, the tetra-anionic H_2TPPS^{4-}. The formation of these aggregates produces a band at around 400 nm at the expense of that at 414 nm corresponding to the Soret band of the monomer (see Fig. 5, dotted line and Table 2). The probability of H_4TPPS^{2-} and H_2TPPS^{4-} to undergo respectively J-aggregation or H-aggregation increases with the concentration of the dye, as can be seen in Fig. 5, inset for the formation of J-aggregates at acidic pH, and/or the presence of positive objects and surfaces, including polyelectrolytes, which may produce a higher local concentration of the dye around these surface as a consequence of the electrostatic attraction.

As deduced from the explanation given above, the aggregative properties of TPPS are related to its acid–base properties. At dilute conditions (10^{-6} M or less) the main species is the monomeric di-anionic H_4TPPS^{2-} at acid pH and the monomeric tetra-anionic H_2TPPS^{4-} at pH higher than 5. At pH close to 5 (Fig. 5, dashed line) both species are present. In order to better observe the transition between the tetra-anionic species and the di-anionic species with the pH, in Fig. 6, the absorbances corresponding to both H_2TPPS^{4-} and H_4TPPS^{2-} species at every pH value have been plotted normalized for their sum, i.e. the sum of the two absorbances is at every pH condition always equal to 1. It can be seen that H_4TPPS^{2-} becomes the main species under pH 4.9 (see Table 2) as stated in the literature [26,41].

As some of the copolymers considered in this study are insoluble in water but dispersible in a mixture of water:DMSO 90:10, the behavior of 10^{-6} M of TPPS in mixtures of water:DMSO has been analyzed. By increasing the volume fraction of DMSO in the mixture, an increasing shift of the H_2TPPS^{4-} monomer band is

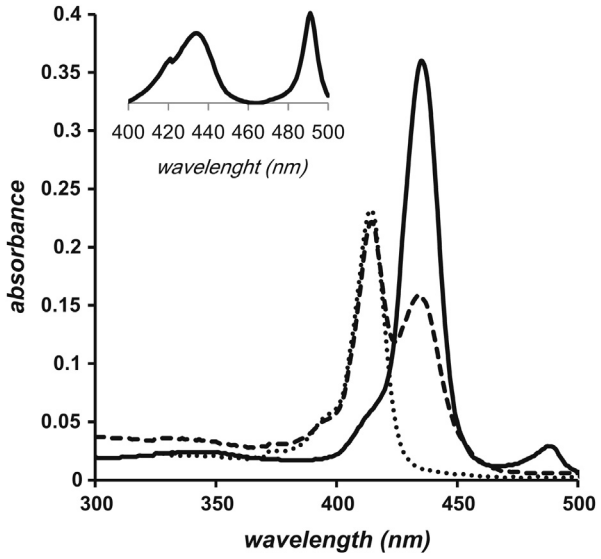

Fig. 5. UV–vis spectra of aqueous solutions containing 10^{-6} M of TPPS at pH 7.15 (dotted line), pH 5.05 (dashed line), pH 1.83 (continuous line); inset: 10^{-4} M of TPPS at pH 2.0.

Table 2
λ_{max} of monomeric H_2TPPS^{4-} and H_4TPPS^{2-} and corresponding transition pH in the presence of $9 \cdot 10^{-5}$ M of the different polymers.

Polymer	Solvent	λ_{max} monomeric H_2TPPS^{4-} (nm)	λ_{max} monomeric H_4TPPS^{2-} (nm)	Transition pH between H_2TPPS^{4-} and H_2TPPS^{4-}
None	H_2O	414	434–435	4.9
None	H_2O:DMSO 90:10	416	437	4.8
PVP	H_2O	421	435	4.3
PVP	H_2O:DMSO 90:10	420	437	4.3
P10	H_2O	423	435	2.1
P10	H_2O:DMSO 90:10	423	437	2.6
P25	H_2O	423	–	1.8
P25	H_2O:DMSO 90:10	423	–	1.6
P50	H_2O:DMSO 90:10	416	437	4.5
P75	H_2O:DMSO 90:10	416	437	4.5
P100	H_2O:DMSO 90:10	416	437	4.5

observed, from 414 to 421 nm, as can be seen in Fig. 7, revealing the solvatochromism of this dye. On the other hand, upon addition of HCl at concentrations of 10^{-3} M or higher, the band corresponding to H_4TPPS^{2-} that in pure water appears at 434–435 nm is also shifted up to 451 nm, the value obtained in pure DMSO, as can be also seen in Fig. 7 and reported in the literature [31]. In mixtures water:DMSO 90:10, both monomeric species experience a shift of the position of their Soret bands by the incorporation of DMSO in relation to the corresponding positions in pure water: that of H_2TPPS^{4-} moves 2 nm to lower energies (from 414 to 416 nm) and that of H_4TPPS^{2-} moves 2–3 nm to lower energies (from 434–435 to 437 nm), as can be read in Table 2. Although not studied here, the H_2TPPS^{4-} becomes more stabilized than H_4TPPS^{2-} when the organic content of the mixtures increases, so that the corresponding protonation constants decrease [31] and thus, the appearance of two extra positive charges in the molecule is prevented. In particular, in mixtures H_2O:DMSO 90:10, a slight shift in the transition pH

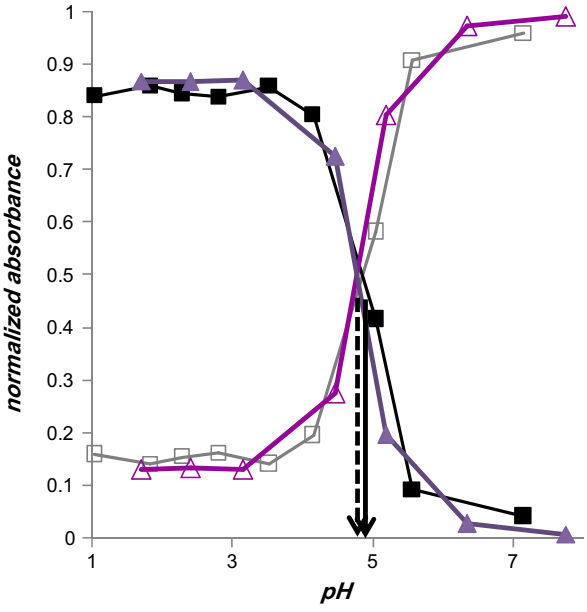

Fig. 6. Absorbances at the λ_{max} of monomeric H_2TPPS^{4-} (414–416 nm) (empty symbols) and at λ_{max} of monomeric H_4TPPS^{2-} (434–437) (filled symbols) as a function of pH, normalized for the sum of both values at each pH of solutions containing 10^{-6} M of TPPS in H_2O (■, □) and in water:DMSO 90:10 (▲, △). The arrows indicate the transition pH between both TPPS species in H_2O (continuous) and in water:DMSO 90:10 (dashed) (see Table 2).

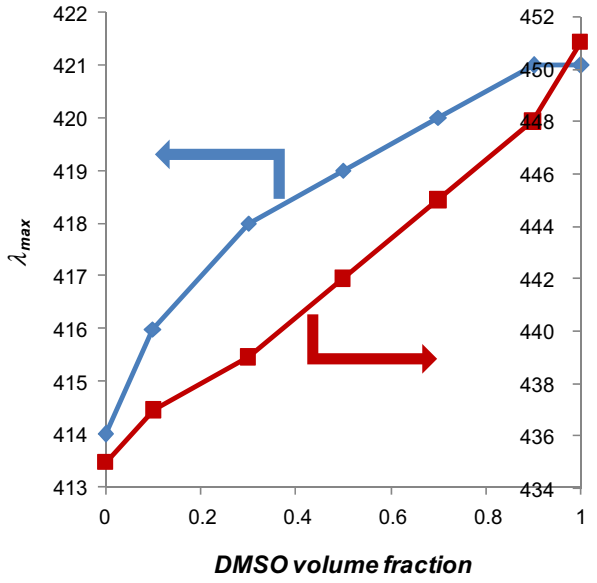

Fig. 7. λ_{max} of absorbance of the monomeric H_2TPPS^{4-} (◆) and the monomeric H_4TPPS^{2-} (■) as a function of the volume fraction of DMSO in the water:DMSO mixtures for solutions containing 10^{-6} M of TPPS.

between the two monomeric forms of the dye at a concentration of 10^{-6} M was found decreasing to approximately pH 4.8, as can be seen in Fig. 6. These changes are related to preferential solvation of TPPS for DMSO in mixtures water:DMSO [31]. As can be seen in Fig. 7, the tendency of H_2TPPS^{4-} to undergo preferential solvation with DMSO is higher than for H_4TPPS^{2-}, so that the corresponding band shift for the former reaches higher relative values than for the latter at low DMSO volume fractions. This is related to the more hydrophilic nature of H_4TPPS^{2-}, which is zwitterionic, thus presenting 6 individual charges.

As can be seen in these studies, environmental conditions of the dyes influence their characteristic absorption bands, as well as their chemical behavior. In particular, band shifting and/or splitting, corresponding to changes in the transition energies and/or excitation/relaxation mechanisms may be observed by UV–vis spectroscopy, and all these properties are related to the polarity of their environment and to the relative probability to stack on other molecules, including self-stacking. Moreover, changes on the acid–base properties of dyes also witness different environmental conditions. The measure of UV–vis spectral changes, and transition pH from tetra-anionic to di-anionic changes, serves to analyze and interpret the environment of TPPS.

3.3. Acid–base properties and band shift of TPPS in the presence of PVP

PVP is an amphiphilic polymer [12,14,15] that lacks of any aromatic or charged functional group, as shown in Fig. 1. Thus, changes on the aggregation and acid–base properties of TPPS must be related to its amphiphilia and/or the π system of the amido group. The amphiphilic behavior for this polymer is related to a compromise of hydrophilic properties associated to the amido groups, and hydrophobic properties associated to the rest of the hydrocarbon chain. Thus, experiments have been done at pH 6 in which the concentration of TPPS is set at 10^{-6} M and the concentration of PVP is varied. At PVP concentrations higher than $9 \cdot 10^{-5}$ M, the presence of the VP units induces a shift of 7 nm of the H_2TPPS^{4-} Soret band from 414 to 421 nm, as can be seen in Fig. 8. These changes may be related to preferential solvation by PVP segments, that is, to specific

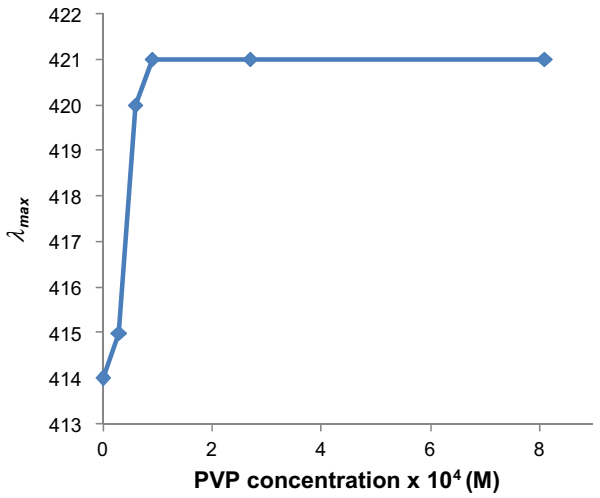

Fig. 8. λ_{max} of absorbance of the monomeric H_2TPPS^{4-} (◆) as a function of the concentration of PVP in water at pH 6 for solutions containing 10^{-6} M of TPPS.

and nonspecific interactions produced by the amphiphilic polymer. On the contrary, the H_4TPPS^{2-} Soret band was not shifted and remained centered at 435 nm (data not shown). The polymeric nature of PVP may provide a less polar local environment for H_2TPPS^{4-} upon preferential solvation at low concentrations of the polymer, and, on the other hand, allows the more hydrophilic H_2TPPS^{4-} to retain its hydration sphere.

Interestingly, it can be seen in Fig. 8 that at concentrations of the polymer lower than $9\cdot10^{-5}$ M, the maximum of absorbance does not reach the plateau at 421 nm. On the contrary, a sharp shift is obtained when increasing the polymer concentration in the range of 10^{-5}–10^{-4} M, such as if a transition between two states was witnessed. It could be related to the formation of polymeric micelles of PVP showing a critical micellar concentration of this order. However, no report in the literature was found about the aggregation and micelle formation of the pristine polymer. A report has been found [45] on the formation of colloidal suspensions by addition of amitriptyline, a tricyclic anti-depressant drug bearing a large π system, to PVP solutions; the drug appears to induce PVP collapse in the form of nanoparticles. Our own assays made by DLS and by fluorescence spectroscopy using 10^{-5} M of pyrene as fluorescent probe, confirm that polymeric micelles are not formed in the range of PVP concentrations between 10^{-6} and 10^{-2} M, even using a PVP of 1,300,000 g/mol of molecular weight (notably higher than the molecular weight of the copolymers, so that aggregation should be enhanced) in the presence and in the absence of 10^{-6} M of TPPS. Then, the transition observed in Fig. 8 may just be related to the probability of PVP segments at these low concentrations to solvate TPPS by means of preferential solvation.

On the other hand, special attention must be paid to PVP solutions at concentrations at which the amount of VP units is coincident with that in the copolymers that will be studied in the following sections. The transition between the two acid and basic monomeric forms also changes as a function of the PVP concentration, as can be seen in Fig. 9(A). At low concentration of the polymer, no shift of the transition pH was observed, and it remained at 4.9. However, at concentrations over $9\cdot10^{-5}$ M, the transition pH is increasingly shifted to lower pH values. Note that there is a correspondence with the shift of the absorption band of the tetra-anionic form of the dye shown in Fig. 8. In the presence of $8.1\cdot10^{-4}$ M of PVP, the transition pH is shifted to a low value such as 3.3. As explained when mixtures of water:DMSO are used as solvent, this may be due to the fact that the hydrophobic environment produced by the polymer stabilizes the basic form in order to prevent the appearance of two extra positive charges in the molecule. Thus, the band shifts of the absorption bands of TPPS, and the changes on the transition pH between H_2TPPS^{4-} and H_4TPPS^{2-} may be related to nonspecific interactions and/or specific interactions that provide preferential solvation of TPPS by the amphiphilic segments of PVP.

Similar behavior is found when the same studies are performed in mixtures water:DMSO 90:10, as can be seen in Fig. 9(B), indicating that the presence of DMSO does not play an additional crucial role on the environment of TPPS in the presence of PVP.

3.4. Acid–base properties and band shift of TPPS in the presence of P10

The UV–vis spectral changes of the dyes in the presence of polyelectrolytes depend on the polymer structure as a whole [28,29]. Hydrophilia, flexibility, degree of ionization of the ionizable groups, presence or absence of aromatic groups, nature and location of functional groups, linear aromatic density, and linear charge density, influence the behavior of the systems and the aggregation state of the dyes. In particular, the presence of charged aromatic groups in the polymer produces strong binding and notorious changes on the dye chemical and spectroscopic behavior. A significant amount of literature shows that the presence of complementary charged polymers produces aggregation of dyes in the form of sandwich-like aggregates [27,28,43,46]. This property has been elegantly used to achieve interesting nanostructures by ionic self-assembly [47–49]. In the case of H_2TPPS^{4-} an intense H-band appears at around 400 nm at the expense of that at 414 nm in the

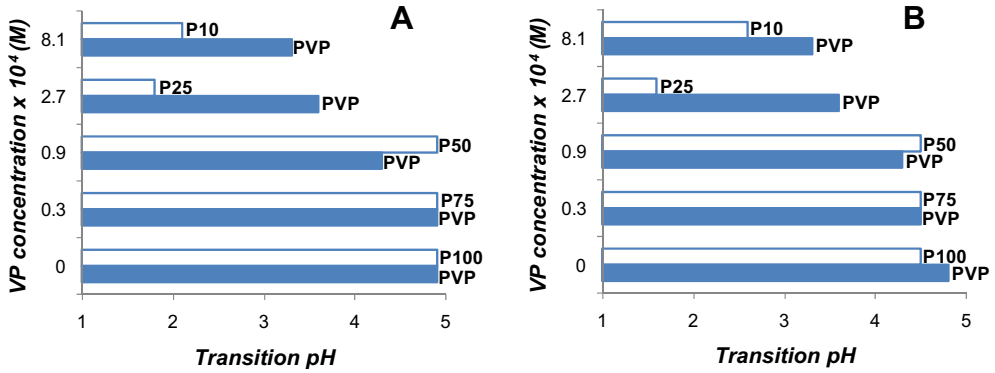

Fig. 9. Transition pH of 10^{-6} M of TPPS in the presence of $9\cdot10^{-5}$ M of the different copolymers or PVP furnishing comparable apparent concentrations of VP in H_2O (A) and water:DMSO 90:10 (B).

presence of poly(allylamine) [42] or CS (as will be shown later) [43]. Besides, the tetra-anionic form is stabilized up to pH 2.2, due to charge neutralization by the polymer. However, when the polyelectrolytes bear positively charged aromatic groups, aromatic–aromatic interactions between these charged aromatic groups and aromatic counterions such as TPPS may compete with the dye self-aggregation. In some cases, as in the presence of poly(4-vinylpyridine) (P4VPy) this interaction becomes intense, and the self-stacking of the dyes is inhibited [26,32,41]. This behavior has been also observed for cationic xanthene dyes and aromatic and aliphatic polyanions [20–22].

The copolymer P10 presents 10% of its pyrrolidones substituted with aromatic amines. As discussed above, the aromatic nature of these substituents may increase the hydrophobia of the copolymer. However, and in particular when the amino groups are charged, they may also enhance the aromatic–aromatic interactions with TPPS. The low linear aromatic density of this polymer may favor its hydration and protonation, and thus its interaction with the dye. As aromatic–aromatic interactions are short-range interactions, close binding between both interacting aromatic residues may produce notorious changes in the absorption characteristics of the dye, due to both unspecific change in polarity and specific aromatic–aromatic interaction. Thus, complexation of 10^{-6} M of TPPS with $9\cdot10^{-5}$ M of P10 produces a shift of 9 nm to lower energies (higher than in pure DMSO) of the corresponding H_2TPPS^{4-} Soret band, as can be seen in Table 2, arising a band at 423 nm, while the H_4TPPS^{2-} Soret band is not shifted, remaining at 435 nm. Interestingly, the transition between H_2TPPS^{4-} and H_4TPPS^{2-} decreases to pH 2.1, as can be also seen in Table 2. Note that at the P10 concentration used in these experiments, the apparent concentration of VP residues is $8.1\cdot10^{-4}$ M. The behavior of TPPS in the presence of a comparable concentration of the homopolymer PVP showed shifts of 7 nm of the H_2TPPS^{4-} Soret band, lower than in the presence of P10 (see Fig. 8), as well as a decrease on the transition pH to 3.3 (see Fig. 9(A)). The higher shifts of these parameters (absorbance maxima and transition pH) in P10 highlight the role of the aromatic amines of the polymers in providing specific interactions with TPPS.

When performing the study in water:DMSO 90:10, it was observed that the H_4TPPS^{2-} Soret band of 10^{-6} M of TPPS moves to 437 nm in the presence of $9\cdot10^{-5}$ M of P10 (Table 2), and the transition pH between both tetra-anionic and di-anionic TPPS species is shifted to 2.6, higher than in the presence of pure water as solvent, but still much lower than for pristine TPPS. As deduced from DLS results shown in Fig. 4, the polymeric chains are in an extended coil form and are highly solvated. Upon preferential solvation of TPPS and of the aromatic amines by DMSO, the close binding between both species may be decreased. Besides, the less polar solvent also contributes to decrease the basicity of the amino groups, decreasing the probability to find them protonated. As said before, in the mixture water:DMSO 90:10, the transition pH of TPPS in the presence of $8.1\cdot10^{-4}$ M of PVP is similar than in water, taking a value of 3.3, as can be seen in Fig. 9(B).

3.5. Acid–base properties and band shift of TPPS in the presence of P25

P25 presents a higher aromatic density than P10. Its solubility in water is decreased at neutral pH, but the polymer is apparently readily soluble by adding HCl so that the basic functional groups may still hydrate and protonate. This is an indication of a still low linear aromatic amine density that provides less compact polymers, although both in H_2O at pH 1 and in mixtures water:DMSO 90:10 at pH 3.5 polymeric aggregation results in the formation of nanoparticles, as was seen in Fig. 4. As a result of the interaction with $9\cdot10^{-5}$ M of this polymer, the tetra-anionic form of TPPS at a concentration of 10^{-6} M is stabilized at least up to pH 1.8 (see Table 2). Whilst the aromatic amine density is increased, the apparent concentration of unmodified pyrrolidones is decreased by comparison with experiments made with P10. However, the H_2TPPS^{4-} Soret band is also shifted to 423 nm as in the case of P10, as can be also seen in Table 2, a fact that may indicate that this notorious shift is mostly provided by the specific aromatic–aromatic interaction between the dye and the aromatic amines. In this respect, the nanoparticles formed with P25 are permeable to TPPS, so that, a strong interaction is observed. The stabilization of the tetra-anionic form may be due to both a higher hydrophobic environment and the charge compensation furnished by the ammonium groups. The apparent VP units concentration for this polymers is $2.7\cdot10^{-4}$ M. Note in Fig. 9(A) that at this concentration of pure PVP, a lower shift of the transition pH is found than in the case of a more concentrated PVP solution, achieving a value of 3.6. However, a higher shift of the transition pH is found for P25 comparing to the case in the presence of P10, related to the increase on the aromatic amine density, provided that the apparent total aromatic amine concentration has been kept constant.

Similar behavior is found in mixtures of water:DMSO 90:10. However, contrarily to the case in the presence of P10, the stabilization of the tetra-anionic form in these conditions is still higher than in pure water, evidenced by a shift of the transition pH between the basic and the acid form to at least pH 1.6, as can be seen in Table 2. This could be related to swelling of DMSO inside the nanoparticles, based on a probable preferential solvation of the polymeric functional groups, that makes the environment inside the particle less polar, and still permeable to TPPS, decreasing also the probability of the dye to protonate. In the mixture water:DMSO 90:10, the transition pH of TPPS in the presence of $2.7\cdot10^{-4}$ M of PVP is comparable to that in water, taking a value of 3.6, as can be seen in Fig. 9(B).

3.6. Acid–base properties and band shift of TPPS in the presence of P50, P75 and P100

None of these polymers are water-soluble, even at acidic conditions. So, the linear aromatic amine density is too high and, as a possible explanation, hydration of the functional groups is prevented by means of a higher probability of these polymers to stabilize stacked planar, non-basic structures in hydrophobic domains. However, suspensions of these polymers at a concentration of $9\cdot10^{-5}$ M and pH 3.5 were obtained by pouring concentrated solutions of the polymers in pure DMSO into 9-fold water volume at the same pH, so that a mixture water:DMSO 90:10 was obtained as solvent. As shown in Fig. 4 and discussed in Section 3.1, the polymers where found in the form of polydisperse microparticles. At these conditions, addition of TPPS produced no effect concerning band shifts in comparison to the situation in the absence of the polyelectrolytes, as can be seen in Table 2. This suggests that the polymers are found in a rather compact, solid form, not permeable to TPPS, with low porosity and hardly solvated by the organic solvent, their amino groups remaining in their basic form, decreasing the probability to undergo aromatic–aromatic interactions with TPPS. The dye may also be stabilized by DMSO upon preferential solvation, and both entities, polymers and dye, behave as practically independent. No effect was found concerning transition pH changes in water, and weak effects are observed in the presence of the microparticles in water:DMSO 90:10, shifting from around 4.8 to around 4.5 in the presence of all polymers, as can be seen in Fig. 9(B).

3.7. Fluorescence studies

Three dimensional graphs regarding excitation and emission wavelengths and intensity are obtained for TPPS in the presence of

different polymers and at different pHs, as shown in Fig. 10. The di-anionic H_4TPPS^{2-} presents an intense emission peak at around 680 nm when excited at 434 nm, while the tetra-anionic species presents two less intense peaks at 642 and 706 nm, when excited around 414 nm (entries A1 and A2, respectively). In the presence of $9{\cdot}10^{-5}$ M of PVP and acidic pH, the peak corresponding to the di-anionic form of TPPS decreases in intensity around two-fold, a fact that may be interpreted as an increase of intersystem crossing from singlet excited states to triplet excited states, provided that triplets are less polar than singlets, and thus they are stabilized in a more hydrophobic environment. This is important for PDT since the energy to produce singlet oxygen is transferred from the triplet state of the photosensitizer. On the other hand, the tetra-anionic form of TPPS presents an intense fluorescence when excited at around 421 nm. The corresponding fluorescence spectrum is wide, and does not present the peak at around 706 nm, while that at 642 nm is shifted to around 650 nm, corresponding to the shift of the absorption band from 414 to 421 nm. The Stokes shift is

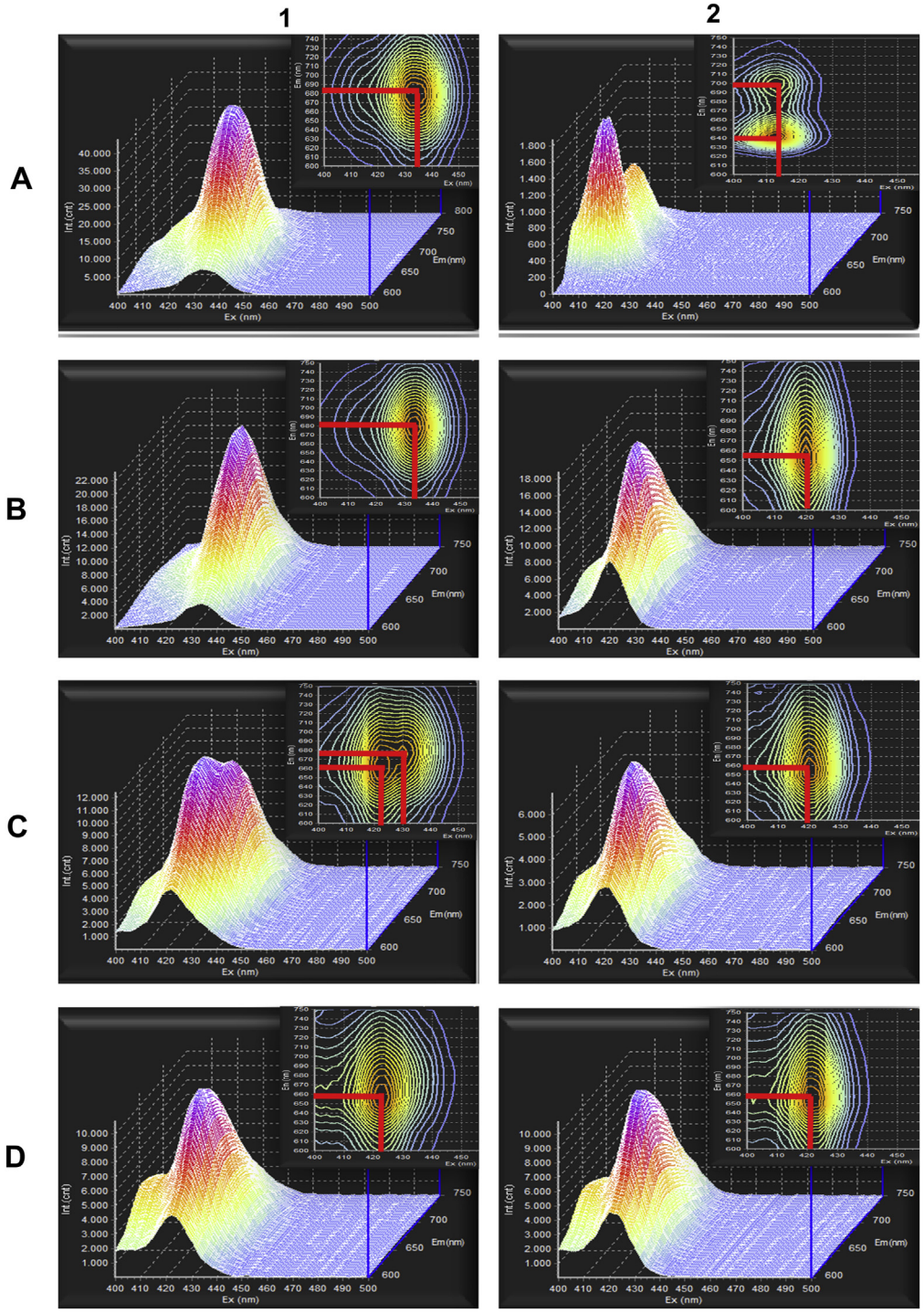

Fig. 10. Three dimensional fluorescence graphs showing fluorescence intensity as a function of excitation and emission wavelengths of 10^{-6} M of TPPS at pH 2 (entries X1) and >5 (entries X2), in the absence of any polymer (entries An), and in the presence of $9{\cdot}10^{-5}$ M of PVP (B1 and B2), P10 (C1 and C2), P25 (D1 and D2).

practically conserved. The intensity of this peak is comparable to that of the di-anionic species. Although not shown here, the same profiles are obtained in the presence of different concentrations of PVP above $9\cdot10^{-5}$ M, while at a concentration of $3\cdot10^{-5}$ M, a profile closer to that of the free monomer is obtained, in correspondence to the band shifts analyzed in Section 3.3 shown in Fig. 8. In the presence of $9\cdot10^{-5}$ M of P10 we can observe that the tetra-anionic species is present at both pH 2 and 5 since emission peaks appear when exciting at 421 nm. The fluorescence peaks of the tetra-anionic form follow the pattern obtained in the presence of PVP, and only a wide emission band appears. At pH 2 a mixture of the di-anionic and the tetra-anionic species is contributing to the fluorescence, the former revealed by the fluorescence peak that appears upon excitation at 435 nm. As the superposition of both bands results in a wide peak, no analysis on the relative intensity will be done. On the contrary, at pH 5, where the tetra-anionic species is the only species present, the corresponding fluorescence intensity is decreased around 3-fold with respect to the case in the presence of PVP. In the presence of P25 the tetra-anionic form is found at both pH 2 and 5, showing a fluorescence intensity higher than in the presence of P10 and lower than in the presence of PVP. Only one emission band is also obtained in this case. Note that at the concentrations used in these studies, the apparent concentration of VP is decreasing in the order PVP < P25 < P10, so that the relative intensity of the fluorescence of TPPS in the presence of these polymers seems to follow the apparent relative concentration of VP, which may furnish the hydrophobic environment to stabilize the triplet state of the dye. On the contrary, the aromatic amine, when protonated, may stabilize the more polar singlet state by means of its own polarity.

3.8. Selective interaction

As highlighted before, the more common behavior of dyes in the presence of complementary charged surfaces, including polyelectrolytes, is the formation of large aggregates based on H-type contacts. This behavior is often due to the nature of the interaction between the dye and the complementary charged surface being electrostatic. Long-range electrostatic interactions produce non-site-specific binding, so that counterions keep their hydration sphere, and locally concentrate near the complementary charged surface [50,51]. In the case of the interaction between dyes and complementary charged polyelectrolytes, the higher local concentration of dyes on the polymeric near environment induces the molecules to self-stack.

Concerning potential biological applications, chitosan (CS) is an interesting polycation. CS is a polysaccharide derived from glucosamine, obtained by partial deacetylation of chitin. Thus, it is a copolymer whose linear charge density, and hence solubility, is modulated by the degree of deacetylation. The CS used in our study presents more than 85% of deacetylated glucosamines that at pH below 5 are protonated, ensuring its easy solubility in water. In the presence of $9\cdot10^{-5}$ M of CS at pH between 3.5 and 5, $1\cdot10^{-6}$ M of TPPS solution in water shows an intense band at around 400 nm corresponding to H-aggregates of H_2TPPS^{4-} formed on the surface of the polyelectrolyte, as can be seen in Fig. 11.

The interaction of dyes with polyelectrolytes bearing complementary charged aromatic groups is more intense than with aliphatic polyelectrolytes, since in the former case, a combination of long-range electrostatic interactions, hydrophobic interactions, and short-range electrostatic interactions may induce strong site-specific binding [22–24,29]. As a consequence of this, in the presence of both types of polycations, TPPS should bind preferentially to the aromatic one. In order to verify this, $1\cdot10^{-6}$ M TPPS solutions have been prepared in the presence of mixtures of CS and P10. P10 was chosen as a readily water-soluble polymer, showing weaker interactions with TPPS than P25, as deduced from the smaller shift of the transition pH. In these experiments, the amount of total polymeric amino groups has been set at $9\cdot10^{-5}$ M, and the relative concentration of CS and P10 has been chosen as variable. In order to increase the probability of P10 to undergo protonation at the very diluted conditions of the experiment, the pH has been set between 3.6 and 3.5. Thus, in Fig. 11 it can be seen that H-aggregation of TPPS is prevented at a CS/P10 ratio of 9:1 and pH 3.5 (dotted line), deduced by the appearance of the sharp band at 423 nm corresponding to the monomeric tetra-anionic form of TPPS complexed by P10. This result highlights the strength and stability of the TPPS/P10 interaction, properties that may be of transcendental importance for biological applications, where different structures presenting different linear and surface charges are found, with potential influence on the state of aggregation of the dye and its consequent response to light.

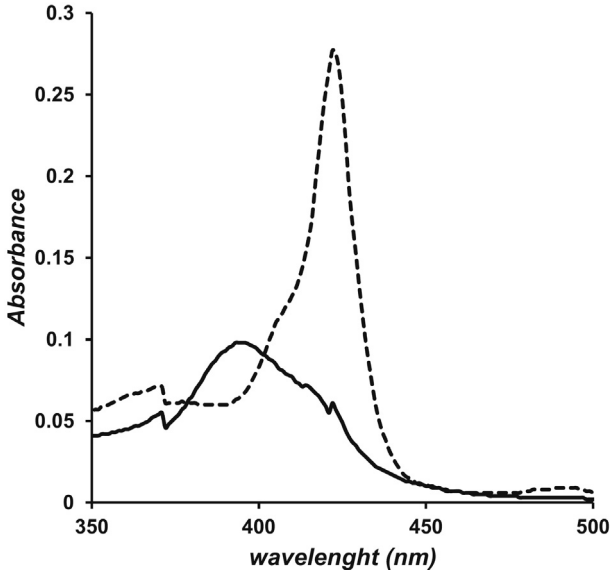

Fig. 11. UV–vis spectra of aqueous solutions containing 10^{-6} M of TPPS in the presence of $9\cdot10^{-5}$ M of CS at pH 3.6 (continuous line), $8.1\cdot10^{-5}$ M of CS and $9\cdot10^{-6}$ M of P10 at pH 3.5 (dashed line).

3.9. TPPS confinement in P25 nano- and micro-particles

The particular characteristics of the copolymers concerning their solubility open the possibility to obtain nanostructures that include TPPS. This can be important for an adequate design of pharmaceutical formulations depending on the possible administration routes. Confinement of a dye in nano- or micro-particles is an adequate strategy to provide stability and improve the targeting. As P25 showed to form nanoparticles with the ability to strongly interact with TPPS, experiments have been done setting the concentration of the polymer at $9\cdot10^{-5}$ M and varying the concentration of TPPS from 0 to $9\cdot10^{-6}$ M. The solvent chosen was water:DMSO 90:10, achieved by pouring 1 volume of a polymer solution of P25 in DMSO with 9 volumes of an aqueous solution of TPPS. The pH selected was 3.5 in order to ensure as much amine protonation as possible, and keep TPPS in its tetra-anionic form. As stated before, in the absence of TPPS, nanoparticles of P25 are formed with an apparent size of 175 nm, showing a low PDI of 0.19, and positive zeta potential. The zeta potential is low (9.23 mV), due to the low charge density of the polymer. By increasing the concentration of TPPS in the samples, a Gaussian-like bell curve

appears when plotting the apparent size of the particles versus the TPPS/P25 ratio, as can be seen in Fig. 12. A maximum appears around a TPPS/P25 ratio of 0.01. There is a correlation of this maximum with an observed change in the sign of the zeta potential. Thus, by increasing the concentration of TPPS up to TPPS/P25 ratio of 0.01, charge neutralization is increasingly achieved, the polymeric chains associate each other forming aggregates whose size also increases, up to around 3 μm, and the zeta potential is increasingly lowered, so that the stabilization effects of the surface charge in the particles are also lowered. Upon adding more TPPS, the absolute value of the negative zeta potential starts increasing. Thus, the particles become more charged, and chain aggregation in the form of large particles is prevented. The apparent size of the particles formed decreases to a plateau at around 150 nm as the TPPS/P25 ratio is decreased. Interestingly, these results show the ability of P25 to confine TPPS, not only by electrostatic interactions, but also by means of additional interactions such as hydrophobic, aromatic–aromatic, and specific interactions with both DMSO and PVP segments.

3.10. Final remarks

The experiments shown in this work highlight the importance of the synthesized PVP derivatives as potential carriers of TPPS for PDT. In this respect, the potential of the synthesized polymers finds its conceptual origin on the biocompatibility of PVP, on its surfactant properties, and, as an absolute novelty of this work, on the incorporation in the polymers of discrete amounts of VP modified with aromatic amines, which increases the hydrophobic properties of the resulting polymers, and provides specific interactions with H_2TPPS^{4-}, resulting in a higher stability of its confinement, and, more interestingly, in the stabilization of the tetra-anionic form in a wide range of pH, avoiding the undesirable self-aggregation both in the form of H- and J-aggregates. Although not shown here, the stability of the confined molecules is extended when different conditions are applied, such as temperatures varying between 10 and 60 °C, and presence of electrolytes such as NaCl at concentrations between 0 and $5\cdot10^{-2}$ M. Among the polymers studied, P10 and P25 exhibit the highest potential due to their solubility, ability to form nanostructures, and ability to incorporate the dye in its tetra-anionic form. These two polymers bear 10 and 25% of modified pyrrolidones, respectively, which results in an advantage under the scope of both low economic and synthetic cost, and retention of biocompatibility. The high affinity of these polymers to bind the dye, by comparison to other biopolymers such as CS, represents an outstanding advantage that may be a first indication of further stability of the assemblies in biological systems. Besides, the low charge of the polymeric systems and their small size are of interest to achieve an effective cellular uptake and permeation through biological cellular membranes.

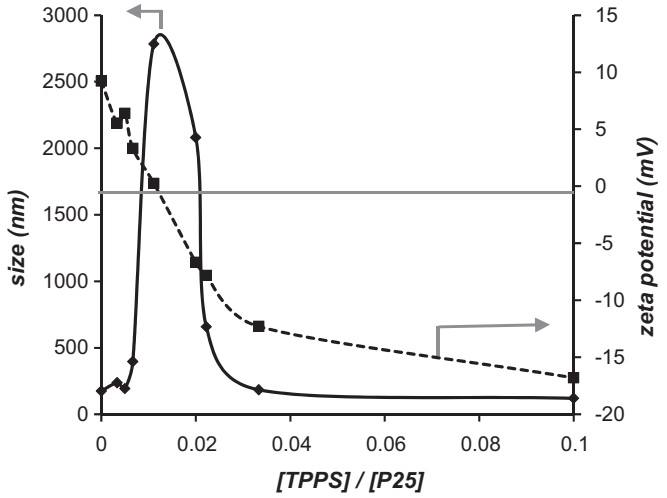

Fig. 12. Apparent size (nm) (left axis) and zeta potential (right axis) of P25 particles in water:DMSO 90:10 at pH 3.5 as a function of the [TPPS]/[P25] ratio. P25 concentration was set at $9\cdot10^{-5}$ M.

4. Conclusions

Copolymers of VP and VP–$ArNH_2$ have been synthesized and their interaction with TPPS has been studied regarding shifts of the absorption bands and shift of the transition pH between the di-anionic and the tetra-anionic form of the dye, both in water and in mixtures water:DMSO 90:10. The interactions with the biocompatible PVP have also been studied as control. The incorporated aromatic amines increase the hydrophobic properties of the resulting polymers and provide specific interactions with TPPS. P50, P75 and P100 resulted insoluble in water, whilst P25 formed polydisperse nanoparticles, and P10 was readily soluble in water. By pouring 1 volume of solutions of P25, P50, P75, and P100 in DMSO into 9 volumes of water, P25 formed nanoparticles of 175 nm, showing a low polydispersity index of 0.19, and a positive zeta potential of 9.23 mV which indicates the effective protonation of some aromatic amino residues. P50, P75, and P100 also formed particles of bigger size and highly polydisperse by this technique. The P25 nanoparticles were permeable to TPPS, which was efficiently confined in them. Both P10 and P25 stabilize the tetra-anionic form of the dye in a wide range of pH, and prevent the undesirable self-aggregation both in the form of H- and J-aggregates. Moreover, the affinity of P10 to bind the dye is higher than for other biopolymers such as CS, which may be a first indication of further stability in biological systems. The low content of modified pyrrolidones in P10 and P25 results in an advantage under the scope of both low economic and synthetic cost, and retention of biocompatibility. All these properties make these polymers interesting materials to confine TPPS in polymeric matrices or micelles as carriers for photodynamic therapy against cancer.

Acknowledgment

The authors thank Fondecyt (Grant Nos. 1090341, 1120514, Chile), FIC-R Los Ríos 2011 (Chile), Grant-in-Aid for Scientific Research (No. 24225003, MEXT, Japan), and Project MAT2010-20001 and Ministerio de Ciencia e Innovación for the FPI Grant (Spain) for financial support.

References

[1] Bonnett R. Photosensitizers of the porphyrin and phthalocyanine series for photodynamic therapy. Chemical Society Reviews 1995;24(1):19–33.
[2] Timoshenko V. Singlet oxygen generation and detection for biomedical applications. In: Baraton M-I, editor. Sensors for environment, health and security. Netherlands: Springer; 2009. p. 295–309.
[3] Dolmans DEJGJ, Fukumura D, Jain RK. Photodynamic therapy for cancer. Nature Reviews Cancer 2003;3(5):380–7.
[4] Niedre MJ, Yu CS, Patterson MS, Wilson BC. Singlet oxygen luminescence as an in vivo photodynamic therapy dose metric: validation in normal mouse skin with topical amino-levulinic acid. British Journal of Cancer 2005;92(2):298–304.
[5] Weishaupt KR, Gomer CJ, Dougherty TJ. Identification of singlet oxygen as the cytotoxic agent in photo-inactivation of a murine tumor. Cancer Research 1976;36(7 Part 1):2326–9.
[6] Tardivo JP, Del Giglio A, de Oliveira CS, Gabrielli DS, Junqueira HC, Tada DB, et al. Methylene blue in photodynamic therapy: from basic mechanisms to clinical applications. Photodiagnosis and Photodynamic Therapy 2005;2(3):175–91.

[7] Shen X, He F, Wu J, Xu GQ, Yao SQ, Xu Q-H. Enhanced two-photon singlet oxygen generation by photosensitizer-doped conjugated polymer nanoparticles. Langmuir 2011;27(5):1739–44.
[8] Li B, Moriyama EH, Li F, Jarvi MT, Allen C, Wilson BC. Diblock copolymer micelles deliver hydrophobic protoporphyrin IX for photodynamic therapy. Photochemistry and Photobiology 2007;83(6):1505–12.
[9] Jang W-D, Nakagishi Y, Nishiyama N, Kawauchi S, Morimoto Y, Kikuchi M, et al. Polyion complex micelles for photodynamic therapy: incorporation of dendritic photosensitizer excitable at long wavelength relevant to improved tissue-penetrating property. Journal of Controlled Release 2006;113(1):73–9.
[10] Ravin HA, Seligman AM, Fine J. Polyvinyl pyrrolidone as a plasma expander. New England Journal of Medicine 1952;247(24):921–9.
[11] Fages E, Pascual J, Fenollar O, García-Sanoguera D, Balart R. Study of antibacterial properties of polypropylene filled with surfactant-coated silver nanoparticles. Polymer Engineering & Science 2011;51(4):804–11.
[12] Cha J, Cui P, Lee J-K. A simple method to synthesize multifunctional silica nanocomposites, NPs@SiO_2, using polyvinylpyrrolidone (PVP) as a mediator. Journal of Materials Chemistry 2010;20(26):5533–7.
[13] Ishii N, Inoue K. Synthesis and regular reflection property of cocoon-like poly(methyl methacrylate) particles by seeded suspension polymerization. Polymer Bulletin 2009;63(5):653–62.
[14] Karagoz B, Gunes D, Bicak N. Preparation of crosslinked poly(2-bromoethyl methacrylate) microspheres and decoration of their surfaces with functional polymer brushes. Macromolecular Chemistry and Physics 2010;211(18):1999–2007.
[15] Minami H, Yoshida K, Okubo M. Preparation of polystyrene particles by dispersion polymerization in an ionic liquid. Macromolecular Rapid Communications 2008;29(7):567–72.
[16] Perrino MP, Navarro R, Tardajos MG, Gallardo A, Reinecke H. A novel route to substituted poly(vinyl pyrrolidone)s via simple functionalization of 1-vinyl-2-pyrrolidone in the 3-position by ring-opening reactions. European Polymer Journal 2010;46(7):1557–62.
[17] Meyer EA, Castellano RK, Diederich F. Interactions with aromatic rings in chemical and biological recognition. Angewandte Chemie International Edition 2003;42(11):1210–50.
[18] Hunter CA, Sanders JKM. The nature of pi–pi interactions. Journal of the American Chemical Society 1990;112(14):5525–34.
[19] Versées W, Loverix S, Vandemeulebroucke A, Geerlings P, Steyaert J. Leaving group activation by aromatic stacking: an alternative to general acid catalysis. Journal of Molecular Biology 2004;338(1):1–6.
[20] Moreno-Villoslada I, Flores ME, Marambio OG, Pizarro GdC, Nishide H. Poly-aromatic-anion behavior of different polyelectrolytes containing benzene-carboxylate units. The Journal of Physical Chemistry B 2010;114(23):7753–9.
[21] Moreno-Villoslada I, Fuenzalida JP, Tripailaf G, Araya-Hermosilla R, Pizarro GdC, Marambio OG, et al. Comparative study of the self-aggregation of rhodamine 6G in the presence of poly(sodium 4-styrenesulfonate), poly(N-phenylmaleimide-co-acrylic acid), poly(styrene-alt-maleic acid), and poly(sodium acrylate). The Journal of Physical Chemistry B 2010;114(37):11983–92.
[22] Moreno-Villoslada I, González F, Arias L, Villatoro JM, Ugarte R, Hess S, et al. Control of C.I. Basic Violet 10 aggregation in aqueous solution by the use of poly(sodium 4-styrenesulfonate). Dyes and Pigments 2009;82(3):401–8.
[23] Moreno-Villoslada I, González R, Hess S, Rivas BL, Shibue T, Nishide H. Complex formation between rhodamine B and poly(sodium 4-styrenesulfonate) studied by ^{1}H-NMR. The Journal of Physical Chemistry B 2006;110(43):21576–81.
[24] Moreno-Villoslada I, Jofré M, Miranda V, Chandía P, González R, Hess S, et al. π-Stacking of rhodamine B onto water-soluble polymers containing aromatic groups. Polymer 2006;47(19):6496–500.
[25] Moreno-Villoslada I, Jofré M, Miranda V, González R, Sotelo T, Hess S, et al. pH dependence of the interaction between rhodamine B and the water-soluble poly(sodium 4-styrenesulfonate). The Journal of Physical Chemistry B 2006;110(24):11809–12.
[26] Moreno-Villoslada I, Murakami T, Nishide H. Comment on "J- and H-aggregates of 5,10,15,20-tetrakis-(4-sulfonatophenyl)-porphyrin and interconversion in PEG-b-P4VP micelles". Biomacromolecules 2009;10(12):3341–2.
[27] Moreno-Villoslada I, Torres C, González F, Shibue T, Nishide H. Binding of methylene blue to polyelectrolytes containing sulfonate groups. Macromolecular Chemistry and Physics 2009;210(13–14):1167–75.
[28] Moreno-Villoslada I, Torres-Gallegos C, Araya-Hermosilla R, Fuenzalida JP, Marambio OG, Pizarro GdC, et al. Different models on binding of aromatic counterions to polyelectrolytes. Molecular Crystals and Liquid Crystals 2010;522(1):136/[436]–147/[447].
[29] Moreno-Villoslada I, Torres-Gallegos Cs, Araya-Hermosilla R, Nishide H. Influence of the linear aromatic density on methylene blue aggregation around polyanions containing sulfonate groups. The Journal of Physical Chemistry B 2010;114(12):4151–8.
[30] Schwab AD, Smith DE, Rich CS, Young ER, Smith WF, de Paula JC. Porphyrin nanorods. The Journal of Physical Chemistry B 2003;107(41):11339–45.
[31] Farajtabar A, Jaberi F, Gharib F. Preferential solvation and solvation shell composition of free base and protonated 5,10,15,20-tetrakis(4-sulfonatophenyl) porphyrin in aqueous organic mixed solvents. Spectrochimica Acta Part A: Molecular and Biomolecular Spectroscopy 2011;83(1):213–20.
[32] Toncelli C, Pino-Pinto JP, Sano N, Picchioni F, Broekhuis AA, Nishide H, et al. Controlling the aggregation of 5,10,15,20-tetrakis-(4-sulfonatophenyl)-porphyrin by the use of polycations derived from polyketones bearing charged aromatic groups. Dyes and Pigments 2013;98(1):51–63. http://dx.doi.org/10.1016/j.dyepig.2013.01.008.
[33] Bryson A. The effects of m-substituents on the pKa values of anilines, and on the stretching frequencies of the N–H bonds. Journal of the American Chemical Society 1960;82(18):4858–62.
[34] Beck-Broichsitter M, Rytting E, Lebhardt T, Wang X, Kissel T. Preparation of nanoparticles by solvent displacement for drug delivery: a shift in the "ouzo region" upon drug loading. European Journal of Pharmaceutical Sciences 2010;41(2):244–53.
[35] Pinto Reis C, Neufeld RJ, Ribeiro AJ, Veiga F. Nanoencapsulation I. Methods for preparation of drug-loaded polymeric nanoparticles. Nanomedicine: Nanotechnology, Biology and Medicine 2006;2(1):8–21.
[36] Kasha M, Rawls HR, Ashraf El-Bayoumi M. The exciton model in molecular spectroscopy. Pure and Applied Chemistry 1965;11(3–4):371–92.
[37] Kemnitz K, Tamai N, Yamazaki I, Nakashima N, Yoshihara K. Fluorescence decays and spectral properties of rhodamine B in submono-, mono-, and multilayer systems. The Journal of Physical Chemistry 1986;90(21):5094–101.
[38] Martínez Martínez V, López Arbeloa F, Bañuelos Prieto J, Arbeloa López T, López Arbeloa I. Characterization of rhodamine 6G aggregates intercalated in solid thin films of laponite clay. 1. Absorption spectroscopy. The Journal of Physical Chemistry B 2004;108(52):20030–7.
[39] Tamai N, Yamazaki T, Yamazaki I, Mizuma A, Mataga N. Excitation energy transfer between dye molecules absorbed on vesicle surface. The Journal of Physical Chemistry 1987;91(13):3503–8.
[40] Maiti NC, Mazumdar S, Periasamy N. J- and H-aggregates of porphyrin–surfactant complexes: time-resolved fluorescence and other spectroscopic studies. The Journal of Physical Chemistry B 1998;102(9):1528–38.
[41] Zhao L, Ma R, Li J, Li Y, An Y, Shi L. Reply to comment on "J- and H-aggregates of 5,10,15,20-tetrakis-(4-sulfonatophenyl)-porphyrin and interconversion in PEG-b-P4VP micelles". Biomacromolecules 2009;10(12):3343–4.
[42] Egawa Y, Hayashida R, Anzai J-i. pH-induced interconversion between J-aggregates and H-aggregates of 5,10,15,20-tetrakis(4-sulfonatophenyl)porphyrin in polyelectrolyte multilayer films. Langmuir 2007;23(26):13146–50.
[43] Synytsya A, Blafkova P, Ederova J, Spevacek J, Slepicka P, Kral V, et al. pH-controlled self-assembling of meso-tetrakis(4-sulfonatophenyl)porphyrin-chitosan complexes. Biomacromolecules 2009;10(5):1067–76.
[44] Ribó JM, Crusats J, Sagués F, Claret J, Rubires R. Chiral sign induction by vortices during the formation of mesophases in stirred solutions. Science 2001;292(5524):2063–6.
[45] Ali MS, Ghosh G, Kabir ud D. Amphiphilic drug persuaded collapse of polyvinylpyrrolidone and poly(ethylene glycol) chains: a dynamic light scattering study. Colloids and Surfaces B: Biointerfaces 2010;75(2):590–4.
[46] Soedjak HS. Colorimetric determination of carrageenans and other anionic hydrocolloids with methylene blue. Analytical Chemistry 1994;66(24):4514–8.
[47] Gröhn F. Electrostatic self-assembly as route to supramolecular structures. Macromolecular Chemistry and Physics 2008;209(22):2295–301.
[48] Ruthard C, Schmidt M, Gröhn F. Porphyrin–polymer networks, worms, and nanorods: pH-triggerable hierarchical self-assembly. Macromolecular Rapid Communications 2011;32(9–10):706–11.
[49] Willerich I, Schindler T, Ritter H, Grohn F. Controlling the size of electrostatically self-assembled nanoparticles with cyclodextrin as external trigger. Soft Matter 2011;7(11):5444–50.
[50] Manning GS. The molecular theory of polyelectrolyte solutions with applications to the electrostatic properties of polynucleotides. Quarterly Reviews of Biophysics 1978;11(02):179–246.
[51] Manning GS. Limiting laws and counterion condensation in polyelectrolyte solutions. 8. Mixtures of counterions, species selectivity, and valence selectivity. The Journal of Physical Chemistry 1984;88(26):6654–61.